Pt-Pt separation.[29] The absence of such an effect for isostructural $Cs[Au(CN)_2]$ strongly suggests that the 1620-cm^{-1} energy gap in $Tl[Au(CN)_2]$ does not correspond to population of a higher vibronic state.

Thermal population (reverse intersystem crossing—the same type of process leading to delayed fluorescence) of the $^1B_{3u}$ (B'_{3u}) state delocalized along the Au(1)-Au(3) chain is a reasonable interpretation of this decrease in lifetime from 100 to 400 K (Figure 2b). The 30-330-ps estimate for the lifetime of this state ($=1/k_3$) is consistent with the value $\tau \leq 300$ ps determined for compounds of $Pt(CN)_4^{2-}$ in which delayed fluorescence is often observed.[29] It is unlikely that the observed decrease in lifetime in this temperature range is a result of a structural change as the structures at 298[12] and 125 K[27] are very similar, and no evidence for a phase transition between these temperatures was found.

Conclusions

The spectroscopic and theoretical results described above for $Tl[Au(CN)_2]$ show that substantial Au-Tl interactions are present in this compound. These interactions influence the energies, intensities, and rates of deactivation of the various states involved in the absorption and luminescence processes. The relatively strong Tl-Au interactions appear to be responsible for the lowering of the absorption and luminescence energies in $Tl[Au(CN)_2]$ relative to $Cs[Au(CN)_2]$.

The isostructural compound $Cs[Au(CN)_2]$ is useful for comparative purposes since no covalent Cs-Au interactions are evident either in its spectroscopic properties or in electronic structure calculations of it. Relativistic effects are demonstrated to play an important role in the Tl-Au interactions by influencing the relative 6s and 6p orbital energies of both Tl and Au.

Acknowledgment. Funds from a DuPont College Science Grant to the Bowdoin Department of Chemistry were used to purchase the laser. We thank Warren Turner and Paul Dolan, Jr., for help with the lifetime measurements, Dale Syphers for help with the magnetic field measurements, and David Roberts for help with data file conversions.

Contribution from the Isotope and Nuclear Chemistry Division and Nuclear Materials Technology Division, Los Alamos National Laboratory, Los Alamos, New Mexico 87545

Extension of Molecular Mechanics to High-Coordinate Metal Complexes. Calculation of the Structures of Aqua and Nitrato Complexes of Lanthanide(III) Metal Ions

Benjamin P. Hay*

Received October 2, 1990

Molecular mechanics methods have been used to calculate the diverse geometries found in 58 known structures of 8- to 12-coordinate aqua- and nitratolanthanide(III) complexes. A simple model based on the replacement of L-M-L bending interactions with nonbonded interactions between the ligand donor atoms and the use of harmonic M-L stretching potentials is shown to yield very reasonable geometric results. A method of structure specification for coordination compounds is presented that allows these calculations to be carried out by using the MM2 program without requiring any software modification.

Molecular mechanics calculations are becoming increasingly important in the area of coordination chemistry.[1] A continuing challenge has been the development of potential functions for metal-ligand interactions that are capable of generating the varied geometries found in d- and f-block metal complexes. Several methods have been devised to obtain the desired structures, but these methods have only been tested on a limited number of low-coordination-number geometries. The aim of the present study was to determine if existing molecular mechanics methodology could be used to calculate the diverse geometries encountered in high-coordinate metal complexes.

The most common method used to specify geometry about the metal ion has been to apply the potential functions of standard organic force fields.[2] Strain-free L-M-L bond angles are defined such that deformations from these strain free values result in an increase in energy. Such conventional force fields have been successfully employed to generate the geometries about the metal in tetrahedral, square-pyramidal, trigonal-bipyramidal, and octahedral Zn(II)[3] and Co(II)[3c] complexes; square-planar and square-pyramidal Cu(II) complexes;[4] square-planar and trigonal-bipyramidal Ni(II) complexes;[5] octahedral complexes of Co(III),[6] Ni(II),[7] and Rh(II);[8] and a hexagonal-bipyramidal complex of Sn(II).[9]

While the conventional approach of defining strain-free L-M-L bond angles is, in theory, applicable to any geometry, it becomes more difficult to implement as the number of ligands increases. The problem is that the number of strain free angles to be defined becomes large, e.g. 21 in a 7-coordinate complexes up to 66 in a 12-coordinate complex. A different set of angles would be required for each of the many possible geometries. In addition, the extent of programming required to ensure the correct assignment of a given strain-free L-M-L angle from a choice of

Table I. Metal-Independent Parameters

bond	k_r, mdyn Å^{-1}	r_0, Å	bond	k_r, mdyn Å^{-1}	r_0, Å
H—O	4.60	0.941	N=O	11.33	1.219
N—O	9.63	1.255			

angle	k_θ, mdyn Å rad^{-2}	θ_0, deg	angle	k_θ, mdyn Å rad^{-2}	θ_0, deg
H—O—H	0.300	109.0	O—N=O	0.700	121.6
H—O—M	0.300	125.5	O—N—M	0.000	0.0
O—N—O	0.700	116.8	out-of-plane about sp^2 nitrogen	0.050	0.0

torsion angle	V_2, kJ/mol	torsion angle	V_2, kJ/mol
O—N—O—M	18.83	O=N—O—M	18.83

nonbonded	ϵ, kJ/mol	d, Å	nonbonded	ϵ, kJ/mol	d, Å
H	0.197	1.50	O(N=O)	0.276	1.74
O(aqua)	0.209	1.74	N	0.230	1.82
O(N—O)	0.209	1.74	M	0.000	2.50

* Correspondence should be addressed to Battelle Pacific Northwest Laboratories, MS K6-81, PO Box 999, Richland, WA 99352.

(1) (a) Brubaker, G. R.; Johnson, D. W. *Coord. Chem. Rev.* **1984**, *53*, 1. (b) Hancock, R. D. *Prog. Inorg. Chem.* **1989**, *36*, 187. (c) Hancock, R. D.; Martell, A. E. *Chem. Rev.* **1989**, *89*, 1875.
(2) (a) Allinger, N. L. *Adv. Phys. Org. Chem.* **1976**, *13*, 1. (b) Burkert, U.; Allinger, N. L. *Molecular Mechanics*; ACS Monograph 177; American Chemical Society: Washington, DC, 1982. (c) Niketic, S. R.; Rasmussen, K. *The Consistent Force Field*; Springer: New York, 1977. (d) Rasmussen, K. *Potential Functions in Conformational Analysis*; Springer: New York, 1985.
(3) (a) Vedani, A.; Dobler, M.; Dunitz, J. D. *J. Comput. Chem.* **1986**, *7*, 701. (b) Vedani, A.; Huhta, D. W.; Jacober, S. P. *J. Am. Chem. Soc.* **1989**, *111*, 4075. (c) Vedani, A.; Huhta, D. W. *J. Am. Chem. Soc.* **1990**, *112*, 4759.

0020-1669/91/1330-2876$02.50/0

possible values increases. For example, in the trigonal-bipyramidal arrangement of an ML_5 complex there are three possible strain-free values for a L–M–L bond angle: 90, 120, and 180°. The program must be coded to assign the correct value to each of the 10 L–M–L bond angles in this complex. As the number of L–M–L bond angles increases, the coding required to accomplish these assignments becomes complex. Given the difficulties in extending the conventional method to high-coordinate metal geometries, an alternative approach is desirable.

Fifty years ago it was recognized that the geometries in many polyatomic molecules could be rationalized in terms of a nonbonding repulsion model.[10] Gillespie proposed that the arrangement of the electron pairs about a central atom could be predicted by considering the distribution of points on the surface of a sphere with an appropriate law of force between the points.[11] Kepert has demonstrated that the points-on-a-sphere repulsion theory is extraordinarily successful in predicting the geometries found in most coordination compounds.[12] This approach has been implemented in molecular mechanics programs by removing L–M–L bending interactions and replacing them with nonbonded interactions between all donor atom pairs. Molecular mechanics models that allow the inner-sphere coordination geometry to be dictated by nonbonded interactions have been successful in generating the structures found in octahedral complexes of Co(III)[13] and Co(II),[13f-h] crown ether complexes of alkali(I)-metal ions,[14] a variety of cyclopentadienyl/X (X = H, Cl, CO) transition-metal complexes,[15] and in two cases, 7-coordinate complexes of lanthanide(III) ions.[16]

In the present study, the latter approach is extended to high-coordinate metal complexes—the 8- to 12-coordinate aqua and nitrato complexes of the lanthanide(III) ions.[17-47] These com-

(4) (a) Brubaker, G. R.; Johnson, D. W. *Inorg. Chem.* **1984**, *23*, 1591. (b) Raos, N.; Simeon, V. *Croat. Chem. Acta* **1983**, *56*, 79; **1984**, *57*, 1217; **1985**, *58*, 127. (c) Sabolovic, J.; Raos, N.; Rasmussen, K. *Croat. Chem. Acta* **1989**, *62*, 495.
(5) Zimmer, M.; Crabtree, R. H. *J. Am. Chem. Soc.* **1990**, *112*, 1062.
(6) (a) Snow, M. R. *J. Am. Chem. Soc.* **1970**, *92*, 3610. (b) Buckingham, D. A.; Maxwell, I. E.; Sargeson, A. M.; Snow, M. R. *J. Am. Chem. Soc.* **1970**, *92*, 3617. (c) Geue, R. J.; Snow, M. R. *J. Chem. Soc. A* **1971**, 2981. (d) Buckingham, D. A.; Sargeson, A. M. *Top. Stereochem.* **1971**, *6*, 219. (e) House, D. A.; Ireland, P. R.; Maxwell, I. E.; Robinson, W. T. *Inorg. Chim. Acta* **1971**, *5*, 397. (f) Snow, M. R. *J. Chem. Soc., Dalton Trans.* **1972**, 1627. (g) Brubaker, G. R.; Euler, R. A. *Inorg. Chem.* **1972**, *11*, 2357. (h) Dwyer, M.; Geue, R. J.; Snow, M. R. *Inorg. Chem.* **1973**, *12*, 2057. (i) DeHayes, L. J.; Busch, D. H. *Inorg. Chem.* **1973**, *12*, 1505, 2011. (j) Niketic, S. R.; Woldbye, F. *Acta Chem. Scand.* **1973**, *27*, 621, 3811. (k) Buckingham, D. A.; Cresswell, P. J.; Dellaca, R. J.; Dwyer, M.; Gainsford, G. J.; Marzilli, L. G.; Maxwell, I. E.; Robinson, W. T.; Sargeson, A. M.; Turnbull, K. R. *J. Am. Chem. Soc.* **1974**, *96*, 1713. (l) Buckingham, D. A.; Dwyer, M.; Gainsford, G. J.; Janson Ho, V.; Marzilli, L. G.; Robinson, W. T.; Sargeson, A. M.; Turnbull, K. R. *Inorg. Chem.* **1975**, *14*, 1793. (m) Yoshikawa, Y. *Bull. Chem. Soc. Jpn.* **1976**, *49*, 159. (n) Niketic, S. R.; Rasmussen, K.; Woldbye, F.; Lifson, S. *Acta Chem. Scand.* **1976**, *A30*, 485. (o) Hald, N. C. P.; Rasmussen, K. *Acta Chem. Scand.* **1978**, *A32*, 753, 879. (p) Niketic, S. R.; Rasmussen, K. *Acta Chem. Scand.* **1978**, *A32*, 391. (q) Laier, T.; Larsen, E. *Acta Chem. Scand.* **1979**, *A33*, 257. (r) Niketic, S. R.; Rasmussen, K. *Acta Chem. Scand.* **1981**, *A35*, 623. (s) Fukuhara, C.; Matsuda, S.; Katsura, K.; Mori, M.; Matsumoto, K.; Ooi, S.; Yoshikawa, Y. *Inorg. Chim. Acta* **1988**, *142*, 203. (t) Schwarz, C. L.; Endicott, J. F. *Inorg. Chem.* **1989**, *28*, 4011. (u) Endicott, J. F.; Kumar, K.; Schwarz, C. L.; Perkovic, M. W.; Lin, W.-K. *J. Am. Chem. Soc.* **1989**, *111*, 7411. (v) Yoshikawa, Y. *J. Comput. Chem.* **1990**, *11*, 326.
(7) (a) McDougall, G. J.; Hancock, R. D.; Boeyens, J. C. A. *J. Chem. Soc., Dalton Trans.* **1978**, 1439. (b) Hancock, R. D.; McDougall, G. J.; Marsicano, F. *Inorg. Chem.* **1979**, *18*, 2847. (c) Hancock, R. D.; McDougall, G. J. *J. Am. Chem. Soc.* **1980**, *102*, 6511. (d) Boeyens, J. C. A. *Acta Crystallogr.* **1983**, *C39*, 846. (e) Boeyens, J. C. A.; Fox, C. C.; Hancock, R. D. *Inorg. Chim. Acta* **1984**, *87*, 1. (f) Adam, K. R.; Brigden, L. G.; Henrick, K.; Lindoy, L. F.; McPartlin, M.; Mimnagh, B.; Tasker, P. A. *J. Chem. Soc., Chem. Commun.* **1985**, 710. (g) Hancock, R. D.; Dobson, S. M.; Evers, A.; Ngwenya, M. P.; Wade, P. W.; Boeyens, J. C. A.; Wainwright, K. P. *J. Am. Chem. Soc.* **1988**, *110*, 2788. (h) Belokon, Yu. N.; Maleev, V. I.; Saporovskaya, M. B.; Bakhmutov, V. I.; Timofeeva, T. V.; Batsanov, A. S.; Struchkov, Yu. T.; Belikov, V. M. *Koord. Khim.* **1988**, *14*, 1565.
(8) (a) Boeyens, J. C. A.; Cotton, F. A.; Han, S. *Inorg. Chem.* **1985**, *24*, 1750. (b) O'Neill, F. M.; Boeyens, J. C. A. *J. Am. Chem. Soc.* **1990**, *29*, 1301.
(9) Drew, M. G. B.; Nicholson, D. G. *J. Chem. Soc., Dalton Trans.* **1986**, 1543.
(10) Sidgwick, N. V.; Powell, H. M. *Proc. R. Soc.* **1940**, *A176*, 153.
(11) (a) Gillespie, R. J.; Nyholm, R. S. *Q. Rev.* **1957**, *11*, 339. (b) Gillespie, R. J. *Can. J. Chem.* **1960**, *38*, 818.
(12) (a) Kepert, D. L. *Prog. Inorg. Chem.* **1977**, *23*, 1; **1978**, *24*, 179; **1979**, *25*, 41. (b) Favas, M. C.; Kepert, D. L. *Prog. Inorg. Chem.* **1980**, *26*, 325; **1981**, *28*, 309.
(13) (a) Hambley, T. W.; Hawkins, C. J.; Palmer, J. A.; Snow, M. R. *Aust. J. Chem.* **1981**, *34*, 45. (b) Hambley, T. W.; Snow, M. R. *Inorg. Chem.* **1986**, *25*, 1387. (c) Coomba, P.; Hambley, T. W.; Zipper, L. *Helv. Chim. Acta* **1988**, 1875. (d) Comba, P. *Inorg. Chem.* **1989**, *28*, 426. (e) Comba, P.; Maeder, M.; Zipper, L. *Helv. Chim. Acta* **1989**, *72*, 1029. (f) Bond, A. M.; Hambley, T. W.; Snow, M. R. *Inorg. Chem.* **1985**, *24*, 1920. (g) Bond, A. M.; Hambley, T. W.; Mann, D. R.; Snow, M. R. *Inorg. Chem.* **1987**, *26*, 2257. (h) Hambley, T. W. *Inorg. Chem.* **1988**, *27*, 2496.
(14) (a) Wipff, G.; Weiner, P.; Kollman, P. *J. Am. Chem. Soc.* **1982**, *104*, 3249. (b) Lifson, S.; Felder, C. E.; Shanzer, A. *J. Am. Chem. Soc.* **1983**, *105*, 3866. (c) Wipff, G.; Kollman, P. *Nouv. J. Chim.* **1985**, *9*, 457. (d) Kollman, P. A.; Wipff, G.; Singh, U. C. *J. Am. Chem. Soc.* **1985**, *107*, 2212. (e) Grootenhuis, P. D. J.; Kollman, P. A. *J. Am. Chem. Soc.* **1989**, *111*, 2152.
(15) Slovokhotov, Yu. L.; Timofeeva, T. V.; Struchkov, Yu. T. *Zh. Struk. Khim.* **1987**, *28*, 3.
(16) Brecknell, D. J.; Raber, D. J.; Ferguson, D. M. *J. Mol. Struct.* **1985**, *124*, 343.
(17) Albertsson, J.; Elding, I. *Acta Crystallogr.* **1977**, *B33*, 1460.
(18) Fitzwater, D. R.; Rundle, R. E. *Z. Kristallogr.* **1959**, *112*, 362.
(19) Hubbard, C. R.; Quicksall, C. O.; Jacobson, R. A. *Acta Crystallogr.* **1974**, *B30*, 2613.
(20) Gerkin, R. E.; Reppart, W. J. *Acta Crystallogr.* **1984**, *C40*, 781.
(21) Harrowfield, J. McB.; Kepert, D. L.; Patrick, J. M.; White, A. H. *Aust. J. Chem.* **1983**, *36*, 483.
(22) Pavia Santos, C. O.; Castellano, E. E.; Machado, L. C.; Vincentini, G. *Inorg. Chim. Acta* **1985**, *110*, 83.
(23) Chatterjee, A.; Maslen, E. N.; Watson, K. J. *Acta Crystallogr.* **1988**, *B44*, 386, 381.
(24) Helmholz, L. *J. Am. Chem. Soc.* **1939**, *61*, 1544.
(25) Sikka, S. K. *Acta Crystallogr.* **1969**, *A25*, 621.
(26) Rogers, R. D. *Inorg. Chim. Acta* **1988**, *149*, 307.
(27) Rogers, R. D.; Voss, E. J. *Inorg. Chim. Acta* **1987**, *133*, 181.
(28) Rogers, R. D. *J. Coord. Chem.* **1988**, *16*, 415.
(29) Rogers, R. D. *Inorg. Chim. Acta* **1987**, *133*, 347.
(30) Bukowska-Strzyzewska, M.; Tosik, A. *Acta Crystallogr.* **1982**, *B38*, 265.
(31) Rogers, R. D.; Kurihara, L. K. *Inorg. Chim. Acta* **1987**, *130*, 131.
(32) Eriksson, B.; Larsson, L. O.; Niinisto, L.; Valkonen, J. *Inorg. Chem.* **1980**, *19*, 1207.
(33) Eriksson, B.; Larsson, L. O.; Niinisto, L.; Valkonen, J. *Acta Chem. Scand.* **1980**, *A34*, 567.
(34) Eriksson, B.; Larsson, L. O.; Niinisto, L. *Acta Chem. Scand.* **1982**, *A36*, 465.
(35) (a) Anderson, M. R.; Jenkin, G. T.; White, J. W. *Acta Crystallogr.* **1977**, *B33*, 3933. (b) Bunzli, J.-C. G.; Pfefferle, J.-M.; Ammann, B.; Chapuis, G.; Zuniga, F.-J. *Helv. Chim. Acta* **1984**, *67*, 1121. (c) Hart, F. A.; Hursthouse, M. B.; Abdul Malik, K. M.; Moorhouse, S. *J. Chem. Soc., Chem. Commun.* **1978**, 549.
(36) Al-Karaghouli, A. R.; Wood, J. S. *J. Chem. Soc., Dalton Trans.* **1973**, 2318.
(37) Milinski, N.; Ribar, B.; Sataric, M. *Cryst. Struct. Commun.* **1980**, *9*, 473.
(38) Zalkin, A.; Forrester, J. D.; Templeton, D. H. *J. Chem. Phys.* **1963**, *39*, 2881.
(39) (a) Fuller, C. C.; Jacobson, R. A. *Cryst. Struct. Commun.* **1976**, *5*, 349. (b) Volodina, G. F.; Rumanova, I. M.; Belov, N. V. *Krystallografiya* **1961**, *6*, 919; **1964**, *5*, 642.
(40) Rogers, D. J.; Taylor, N. J.; Toogood, G. E. *Acta Crystallogr.* **1983**, *C39*, 939.
(41) Benetollo, F.; Bombieri, G.; Cassol, A.; De Paoli, G.; Legendziewicz, J. *Inorg. Chim. Acta* **1985**, *110*, 7.
(42) Bunzli, J.-C. G.; Klein, B.; Wessner, D.; Schenk, K. J.; Chapuis, G.; Bombieri, G.; De Paoli, G. *Inorg. Chim. Acta* **1981**, *54*, L43.
(43) Burns, J. H. *Inorg. Chem.* **1979**, *18*, 3045.
(44) Backer-Dirks, J. D.; Cooke, J. E.; Galas, A. M. R.; Ghotra, J. S.; Gray, C. J.; Hart, F. A.; Hursthouse, M. B. *J. Chem. Soc., Dalton Trans.* **1980**, 2191.
(45) Tomat, G.; Valle, G.; Di Bernardo, P.; Zanonato, P. L. *Inorg. Chim. Acta* **1985**, *110*, 113.
(46) Toogood, G.; Chieh, C. *Can. J. Chem.* **1975**, *53*, 831.
(47) Sherry, E. G. *J. Inorg. Nucl. Chem.* **1978**, *40*, 257.

plexes were chosen because the 58 available X-ray structures represent 14 different geometries and, thus, would provide a thorough test of the method. Ligand types were intentionally limited to the aqua and nitrato groups in order to minimize the size of the required parameter set. In what follows it is demonstrated that the specification of metal–ligand interactions in terms of nonbonded interactions between donor atoms yields a force field that allows the calculation of these structures.

Methods

Potential Energy Functions. The program used to carry out the molecular mechanics calculations was Allinger's MM2.[48] The potential energy expression was restricted to the sum of four terms, which have been utilized in the majority of prior work on metal complexes.[1]

$$U = \sum(E_r + E_\theta + E_\phi + E_{nb})$$

$$E_r = \tfrac{1}{2}k_r(r - r_0)^2$$

$$E_\theta = \tfrac{1}{2}k_\theta(\theta - \theta_0)^2$$

$$E_\phi = \tfrac{1}{2}V_2(1 - \cos 2\phi)$$

$$E_{nb} = A \exp(-Bd) - C/d^6$$

$$A = 2.9 \times 10^5\epsilon^*$$

$$B = 12.5/d^*$$

$$C = 2.25\epsilon^* d^{*6}$$

E_r gives the stretching energy arising from bond length deformations. E_θ gives the bending energy arising from bond angle deformations and out-of-plane bending.[48b] In this work, out-of-plane bending interactions were only included for the nitrate nitrogen. E_ϕ gives the torsional energy arising from rotation about bonds. E_{nb} gives the nonbonded interaction energy arising from van der Waals interactions between atom pairs. For a given atom pair type, the nonbonded parameters A, B, and C are generated from values of ϵ^* and d^*, which, in turn, are obtained from the expressions $\epsilon^* = (\epsilon_i\epsilon_j)^{1/2}$ and $d^* = d_i + d_j$. This selection of potential energy functions can be implemented within the MM2 program through a choice of options in the input file for each run. Complete tables of the k_r, r_0, k_θ, θ_0, V_i, ϵ_i, and d_i values used in this work are given below.

An alternate method for defining the structure of a metal complex was employed in order to achieve the required number of attachments and the desired interactions at the metal. Rather than attachment of all the ligands to a single metal center, each ligand donor atom (L) is attached to a separate metal atom. These monoligated metals are then superimposed to yield the desired structure. This approach results in the replacement of L–M–L bending interactions by L--L nonbonded interactions. The replacement stems from the fact that no two donor atoms are actually attached to the same metal atom and, thus, L–M–L angles are not perceived to be present by MM2. Since the program computes nonbonded interactions between all atom pairs that are not bound to one another or to a common atom, nonbonded interactions are computed for the donor atom pairs. An exception arises only when the pair shares a common atom, e.g., the two oxygen donors in the same nitrato ligand. In such a case, the separation of the geminal oxygens is predominantly dictated by bond length and bond angle preferences within the nitrate group .

In practice, the monoligated metals which make up a metal complex are positioned such that they are almost, but not exactly, coincident. This is accomplished by starting with all metal atoms at the origin and then offsetting them from one another by adding or subtracting increments of 0.000 01 Å to or from their x, y, and/or z coordinates such that no two metals have an identical coordinate set. The reason for these slight offsets is that exact superpositioning causes program execution to halt due to division by zero, a problem that arises as the program attempts to compute metal–metal nonbonded interactions.

After metal atom coordinates have been assigned, the motion of each metal atom is restricted in all directions in order to keep the cluster from drifting apart during the minimization process. For proper performance of the restricted motion algorithm, it is necessary that none of the metal atoms be at the end of an atom chain. Therefore, the connectivity list is edited such that the metal atoms are attached to one another in a ring formation.

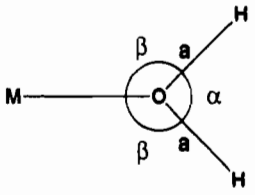

a = 0.940 ± 0.043 Å
α = 109.5 ± 2.4°
β = 123.3 ± 1.6°

Figure 1. Average geometry of the aqua ligand.

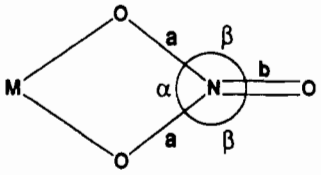

a = 1.255 ± 0.008 Å
b = 1.219 ± 0.009 Å
α = 116.8 ± 1.0°
β = 121.6 ± 0.5°

Figure 2. Average geometry of the nitrato ligand.

Defining the structure in this manner introduces some unwanted interactions into the calculations. They are zeroed by the appropriate choice of parameters: M–M bonds are assigned k_r values of 0 mdyn Å^{-2}, M–M–M and M–M–L bond angles are assigned k_θ values of 0 mdyne Å rad^{-2}, torsions about M–M bonds are assigned V_i values of 0 kJ/mol, and any nonbonded interactions involving an M atom are removed by assigning $\epsilon = 0$ for the metal atom.

In calculations that have been performed on other metal complexes, M–L torsions are generally not included in the strain energy expression because of the high periodicity and lower barriers of the rotations about M–L bonds.[1] Such torsions were omitted in this study by setting all torsional barriers for rotation about M–L bonds to zero.

An example MM2 input file is available (supplementary material).

Initial Input Coordinates. The calculations require an assumed initial geometry for the complex expressed in terms of Cartesian coordinates. The initial coordinates were derived in one of two ways. First, Cartesian coordinates were calculated from available fractional crystal coordinates. In cases where the fractional coordinates for the hydrogen atoms were not given, they were positioned as indicated by the hydrogen-bonding networks in the lattice. This was accomplished with the molecular editing features of the graphics program Chem3D Plus.[49] Second, an alternate approach was to obtain a crude set of Cartesian coordinates from a three-dimensional representation created entirely with Chem3D Plus. Since many of the complexes have the potential for more than one structural isomer, care was taken to ensure that the ligands were oriented as in the observed structure. Calculated structures from both types of input were generated for all of the complexes examined in this study. Without exception, the crude Chem3D Plus starting geometry and the fractional coordinate starting geometry yield identical outputs. The fact that the same final geometry can be obtained from different starting points establishes a calculated structure to be a minimum on the potential surface.

Parametrization. Metal-Independent Parameters. Table I gives the metal independent portion of the parameter set used in this work. Values of k_r, k_θ, and V_i were chosen to be consistent with the existing MM2 parameter set. Ideal bond lengths (r_0) and bond angles (θ_0) were chosen to reproduce observed average geometries of the aqua and nitrato ligands.

Structural data for the aqua ligand were limited to neutron diffraction data for three nonaaqualanthanide(III) ions.[19,23,25] These structures reveal that the aqua ligand coordinates with an approximate trigonal-planar geometry. The average H–O bond length and the average bond angles about the oxygen are summarized in Figure 1. The relatively large standard deviations in these values reflect a variability in geometry,

(48) (a) Allinger, N. L.; Yuh, Y. H. QCPE Program No. 395, Quantum Chemistry Program Exchange. Indiana University Chemistry Department, Indiana, 1977; modified version 1980. (b) The definition of the out-of-plane bending angle is given in: Allinger, N. L.; Tribble, M. T.; Miller, M. A. *Tetrahedron* **1972**, *28*, 1173.

(49) Rubenstein, M.; Rubenstein, S. Cambridge Scientific Computing, Inc., Cambridge, MA, 1989.

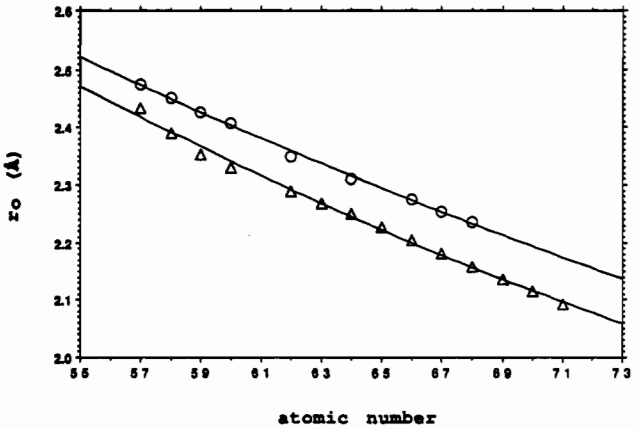

Figure 3. Plots of r_0 vs atomic number for M–O_{aqua} (△) and M–O_{nit} (nit = nitrato) (○) bonds.

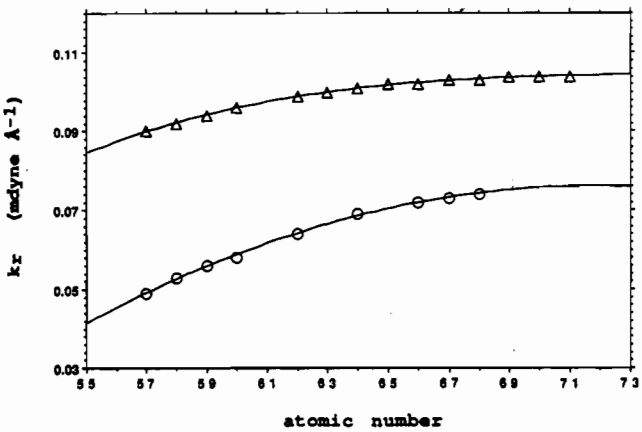

Figure 4. Plots of k_r vs atomic number for M–O_{aqua} (△) and M–O_{nit} (○) bonds.

which can be attributed largely to distortions arising through hydrogen bonding in the lattice. The θ_0 values for the angles about oxygen were chosen to enforce a geometry where all three aqua atoms are coplanar with the metal atom.

X-ray data for 70 nitrato ligands in 19 structures[32-47] were averaged, and the resulting bond lengths and angles are summarized in Figure 2. The observed strict planarity of the nitrato ligand is maintained in calculated structures by three types of interaction: the sum of θ_0 values about the nitrogen is 360°, torsional interactions about the N–O bonds have minima at 0 and 180°, and the out-of-plane bending about the N atom is at a minimum when the oxygens are coplanar with nitrogen. The force constants for M–O–N bending interactions were set to zero.

The nonbonded parameters, ϵ and d, were taken directly from the MM2 parameter set where possible. Nonbonded interactions between any atom–metal pair were omitted by setting all metal ϵ values to zero. In the MM2 program, H–C bonds are shortened to 0.915 of their length by moving the hydrogen in toward the carbon prior to calculating nonbonded interactions between any atom–hydrogen pairs. This is done to place the center of hydrogen repulsion closer to the actual position of electron density.[50] The same foreshortening of H–O bonds was employed in this study by assigning the aqua hydrogen to atom type 5.

Metal-Dependent Parameters. Following the assignment of the metal-independent parameters presented in Table I, the only missing parameters were the M–O stretching constants, k_r and r_0. Initial estimates of these metal-dependent parameters were adjusted to yield the best agreement between calculated and observed M–O bond lengths for available aqua and nitrato complexes. These adjustments were accomplished through manual inspection. For each M–O bond type, the discrepancies between the calculated and observed bond lengths were examined in all complexes which contained that bond type and the parameters were adjusted in such a way as to minimize those discrepancies. Successive iterations yielded the M–O stretching constants given in Table II. Plots of r_0 vs atomic number (Figure 3) and k_r vs atomic number (Figure 4) revealed expected trends upon moving across the lanthanide series from La to Lu; i.e., a decrease in r_0 and an increase in k_r accompany the shift to smaller metals with lower size to charge ratios. These plots allow the estimation of M–O stretching parameters in cases where there was a lack of structural data.

(50) Allinger, N. L. *J. Am. Chem. Soc.* **1977**, *99*, 8127.

Table II. Metal-Dependent Parameters[a]

metal(III) ion	M–O_{aqua}		M–O_{nit}[b]	
	k_r, mdyn Å^{-1}	r_0, Å	k_r, mdyn Å^{-1}	r_0, Å
La	0.090	2.434	0.049	2.475
Ce	0.092	2.390	0.053	2.451
Pr	0.094	2.353	0.056	2.427
Nd	0.096	2.330	0.058	2.407
Pm	[0.098]	[2.317]	[0.062]	[2.380]
Sm	0.099	2.289	0.064	2.350
Eu	0.100	2.269	[0.067]	[2.338]
Gd	0.101	2.250	0.069	2.310
Tb	0.102	2.227	[0.071]	[2.295]
Dy	0.102	2.040	0.072	2.275
Ho	0.103	2.181	0.073	2.255
Er	0.103	2.158	0.074	2.237
Tm	0.104	2.136	[0.075]	[2.215]
Yb	0.104	2.114	[0.076]	[2.195]
Lu	0.104	2.092	[0.076]	[2.175]

[a] Brackets indicate parameters that were estimated from plots of k_r and r_0 vs atomic number. [b] Nit = nitrato.

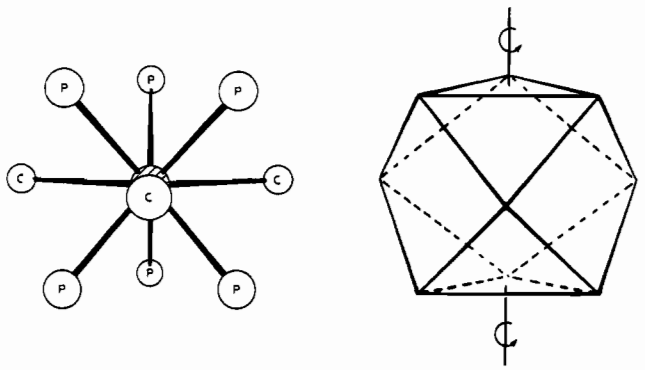

Figure 5. Geometry of an ideal tricapped trigonal prism.

Comparison of Calculated and Observed Structures

The principal objective of the present work was to test the ability of a simple force field to generate the geometries of the 8- to 12-coordinate aqua and nitrato complexes of the lanthanide(III) metal ions. In the following discussion, the calculated structures are compared to the observed structures for these complexes. It is emphasized that the calculated structures do not necessarily represent the most stable arrangement of ligands but merely the arrangement of ligands most closely resembling the observed structures. Attempts to locate energy minima representing possible structural isomers for these complexes are limited only to the cases where crystallographic data on such isomers are available.

The strain energies associated with each complex are also reported. Given the harmonic stretching and bending potentials used in this model and the uncertainty concerning the correct form of the potential function for the repulsions between ligand donor atoms, these energies must be viewed as approximate in value. Nevertheless, the results obtained in other studies[12-16] strongly suggest that these approximate strain energies can be used to identify the more stable arrangement of ligands when more than one isomer exists. This approach is employed here to assign the relative stability to the two structures observed for the nonaaqua, octaaqua, $M(NO_3)_3(OH_2)_3$, $M(NO_3)_5(OH_2)^{2-}$, and $M(NO_3)_5(OH_2)_2^{2-}$ complexes.

(i) The Nonaaqua Ion. The structures of the lanthanide(III) hydrates, $M(OH_2)_9X_3$, have been extensively investigated, and X-ray data are available for every nonaaqua complex, except Pm, over the series La to Lu. The data consist of 38 structures that can be classified by counterion into three groups: counterion (number of structures); ethyl sulfates (19);[17-20] triflates (15);[21-23] bromates (4).[17,24,25] In addition, a nonaaqua ion is observed in the structure $[Nd(OH_2)_9]Cl_3 \cdot 15\text{-crown-}5 \cdot H_2O$.[26]

Table III. Comparison of Calculated and Observed M–O Bond Lengths (Å) and Selected Angles (deg) in Representative $M(OH_2)_9X_3$ Complexes (X = OTf^- and $EtSO_4^-$)

metal ion (counterion)	M–O_c	M–O_p	M–O_c/M–O_p	O_p–M–O_p[a]	O_p–M–O_c[b]	θ[c]	strain energy, kJ/mol	ref
La (calcd)	2.615	2.515	1.040	76.9	69.0	45.9	−21.05	
La (OTf^-)	2.619	2.519	1.040	75.6	69.2	45.5		21
La ($EtSO_4^-$)	2.616	2.517	1.039	76.3	69.3	45.0		20
La ($EtSO_4^-$)	2.611	2.513	1.039					23
Nd (calcd)	2.575	2.455	1.049	77.4	68.9	46.2	−13.39	
Nd (OTf^-)	2.572	2.469	1.042	75.7	69.3	45.1		23
Nd (OTf^-)	2.568	2.451	1.048	75.1	69.4	44.8		22
Nd ($EtSO_4^-$)	2.570	2.457	1.046	75.5	69.3	45.1		20
Gd (calcd)	2.547	2.413	1.056	77.6	68.8	46.3	−4.94	
Gd (OTf^-)	2.546	2.402	1.060	75.3	69.4	44.8		21
Gd ($EtSO_4^-$)	2.536	2.401	1.056	75.3	69.4	44.9		20
Gd ($EtSO_4^-$)	2.536	2.395	1.059					23
Ho (calcd)	2.527	2.380	1.062	77.8	68.7	46.5	4.06	
Ho (OTf^-)	2.526	2.367	1.067	75.3	69.3	44.9		22
Ho ($EtSO_4^-$)	2.511	2.362	1.061	75.0	69.5	44.7		20
Ho ($EtSO_4^-$)	2.511	2.391	1.050	75.5	69.4	44.9		19
Lu (calcd)	2.505	2.341	1.070	78.1	68.7	46.7	17.99	
Lu (OTf^-)	2.503	2.291	1.093	76.1	69.2	45.4		21
Lu ($EtSO_4^-$)	2.497	2.318	1.077	75.3	69.4	44.9		20
Lu ($EtSO_4^-$)	2.519	2.287	1.101					23

[a] Average of the six angles made by adjacent O_p atoms within the triangular faces of the prism. [b] Average of the 12 acute angles made by O_p and neighboring O_c atoms. [c] Average of the six angles made by M–O_p bonds and the C_3 axis.

These complexes all exhibit tricapped trigonal prismatic (TCTP) geometries. In the ideal TCTP geometry shown in Figure 5 there are six equivalent positions (O_p) at the vertices of a regular trigonal prism and three equivalent positions (O_c), which cap the rectangular faces of this prism. Although the inner coordination sphere geometry of all the nonaaqua ions is similar, there are counterion-dependent structural differences that have been attributed to hydrogen-bonding networks present in the crystal lattice.[17,21] In the following discussion the structures are classified into two types, the ethyl sulfate and triflate type and the bromate type.

In the ethyl sulfate and triflate type of structure the six O_p atoms form a regular trigonal prism. The three O_c atoms lie in the mirror plane, but the equilateral triangle that they form is rotated about the C_3 axis by 4–5° from the D_{3h} position of an ideal TCTP geometry, resulting in C_{3h} symmetry. The M–O_p bonds are shorter than the M–O_c bonds. The M–O_c/M–O_p bond length ratio ranges from 1.04 for La up to 1.10 for Lu. The hydrogens are oriented as shown in Figure 6, where the H–O_c–H planes contain the C_3 axis and a 40–45° rotation about the M–O_p bonds is required to place the H–O_p–H planes coplanar with the C_3 axis.

The difference between the M–O_p and M–O_c bond lengths observed in these complexes has been explained previously in terms of points-on-a-sphere repulsion calculations.[21] In the minimum energy TCTP geometry obtained by those calculations, the four nearest-neighbor interligand distances for a capping ligand were, on average, shorter than those for a prismatic ligand. This observation led to the prediction that the capping ligands experience an excess steric repulsion over that of the prismatic ligands, which should be alleviated by lengthening the metal to capping ligand bonds. As the molecular mechanics approach allows M–O bond lengths to change, a feature not present in the points-on-a-sphere model, it was hoped that the observed M–O_c/M–O_p ratios would be duplicated in the MM2 calculations.

Calculation of the structure of a nonaaqua metal ion yields a regular TCTP geometry of D_{3h} symmetry as the minimum energy conformation of the oxygen atoms. This calculated conformation, shown in Figure 6, is similar to the observed structures in that both contain regular trigonal prisms and both have identical capping hydrogen orientations but differs from the observed structures in the positioning of the O_c atoms and the orientation of the prismatic hydrogens. In the calculated structure a 2–3° rotation about the M–O_p bonds, vs a 40–45° rotation in the observed structures, is needed to place the H–O_p–H planes coplanar with the C_3 axis. These structural differences represent

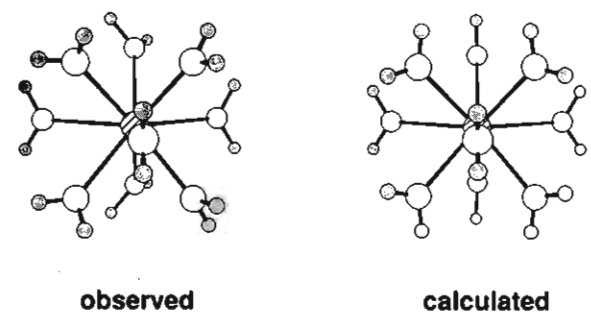

Figure 6. Observed ethyl sulfate and triflate structures and the calculated lowest energy structure for the nonaaqua ion.

distortions from the calculated conformation, which occur to achieve optimum hydrogen bonding in the crystal lattice.

Comparisons of selected observed and calculated structural features for representative members of the lanthanide series are given in Table III. With the exception of Lu, the calculations were found to reproduce the observed M–O_p and M–O_c bond lengths to within ±0.02 Å and O–M–O bond angles to within ±3° over the entire lanthanide series. The appreciable scatter in the observed Lu values may be due, in part, to experimental difficulties encountered during data collection, as the $Lu(OH_2)_9^{3+}$ ion is not stable and the crystals tend to lose water.[21,23] The best agreement is with the Lu structure, which was obtained at 171 K.[20] Examination of the strain energies for these complexes shows an increase of ~39 kJ/mol from La to Lu due to the increasingly unfavorable oxygen–oxygen steric interactions as the size of the metal atom decreases.

A significantly altered structure is observed for the nonaaqua ion when the counterions are bromates. The coordination geometry is an ideal TCTP one of D_{3h} symmetry. On average, the M–O_c bond lengths are 0.06 Å shorter and the M–O_p bond lengths are 0.02 Å longer than those observed in the corresponding ethyl sulfate and triflate structures, resulting in lower M–O_c/M–O_p ratios for the bromate structures. All the hydrogens are positioned such that a 90° rotation about the M–O bonds is required to place the H–O–H planes coplanar with the C_3 axis (see Figure 7).

Attempts to minimize the conformation seen with the bromate counterions of the nonaaqua ion failed when the crystal structure was used to provide the input coordinates. A D_{3d}, rather than the desired D_{3h}, symmetry was obtained due to rotations about the M–O_p bonds. However, it was possible to reproduce the

Table IV. Comparison of Calculated and Observed M–O Bond Lengths (Å) and Selected Angles (deg) in $M(OH_2)_9(BrO_3)_3$ Complexes[a]

metal ion	M–O_c	M–O_p	M–O_c/M–O_p	O_p–M–O_p[b]	O_p–M–O_c[c]	θ[d]	strain energy, kJ/mol	ref
Pr (calcd)	2.55	2.53	1.008	72.5	70.0	43.1	−10.04	
Pr (obsd)	2.52	2.49	1.013	79.1	68.4	47.4		17
	[2.59]	[2.47]	[1.047]	[75.6]	[69.3]	[45.3]		17, 18, 20
Nd (calcd)	2.54	2.52	1.009	72.5	70.0	43.1	−7.57	
Nd (obsd)	2.51	2.47	1.016					24
	[2.57]	[2.46]	[1.045]	[75.4]	[69.3]	[44.9]		20, 22, 23
Sm (calcd)	2.52	2.50	1.009	72.6	70.0	43.2	−2.68	
Sm (obsd)	2.55	2.46	1.037	78.8	68.5	47.2		25
	[2.55]	[2.42]	[1.052]	[75.3]	[69.4]	[45.1]		20
Yb (calcd)	2.46	2.43	1.012	72.9	70.0	43.3	24.60	
Yb (obsd)	2.43	2.32	1.047	79.4	68.3	47.5		17
	[2.52]	[2.32]	[1.087]	[75.5]	[69.3]	[45.0]		17, 20

[a] Values given in brackets are the average distances and angles observed in the corresponding triflate and ethyl sulfate structures. [b] Average of the six angles made by adjacent O_p atoms within the triangular faces of the prism. [c] Average of the 12 acute angles made by O_p and neighboring O_c atoms. [d] Average of the six angles made by M–O_p bonds and the C_3 axis.

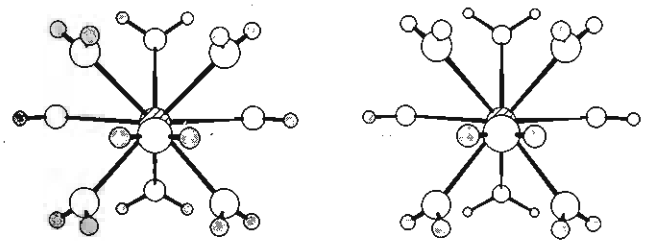

Figure 7. Observed and calculated bromate structures for the nonaaqua ion.

hydrogen atom orientation of the bromate structure by imposing symmetry constraints. A single prismatic hydrogen was used to define the positions of the 11 other prismatic hydrogens. All other atoms in the molecule were left unconstrained. The resulting calculated structure, shown in Figure 7, resembles the observed structures in that it contains a regular TCTP geometry of D_{3h} symmetry and has the desired hydrogen orientation but differs from the observed structure in that the calculated structure is less compressed along the C_3 axis. As with the ethyl sulfates and triflates, the difference between the observed and calculated structures may be attributed to hydrogen bonding present in the crystal lattice. Two oxygens of each bromate anion are hydrogen bonded to two prismatic and two capping hydrogens in such a way that the prismatic oxygens are displaced toward the plane of the capping oxygens, resulting in the observed compression along the C_3 axis.[21]

Comparisons of selected observed and calculated structural features for the four known bromate complexes are given in Table IV. The calculated bromate conformations lie 4–8 kJ/mol higher in energy than the corresponding ethyl sulfate/triflate conformations. It can be seen that forcing the hydrogens into an unfavorable orientation results in a change in M–O bond lengths. As in the observed bromate structures, the M–O_c bonds are shorter and the M–O_p bonds are longer than those observed in the corresponding ethyl sulfate and triflate structures. The calculated M–O_c lengths are within ±0.03 Å of the observed values, but the calculated M–O_p lengths are, on average, 0.06 Å too long.

(ii) The Octaaqua Ion. Unlike the nonaaqua complexes, the octaaqua ions exhibit more than one coordination geometry.[27-31] The majority of the polyhedra in these complexes are described as being close to one of the expected geometries for eight-coordination, i.e. either a square antiprism or a dodecahedron.[51] The polyhedron that is formed is apparently dictated by the packing environment and the hydrogen-bonding network present within a given lattice. Both the square-antiprism and dodecahedron geometries were obtained in the calculations. While the square-antiprism geometry was readily located, the dodecahedral geometry was obtained for the octaaqua ions only by imposing symmetry constraints. Since hydrogen atom positions are not reported for the observed structures, only inner-sphere coordination geometries are compared.

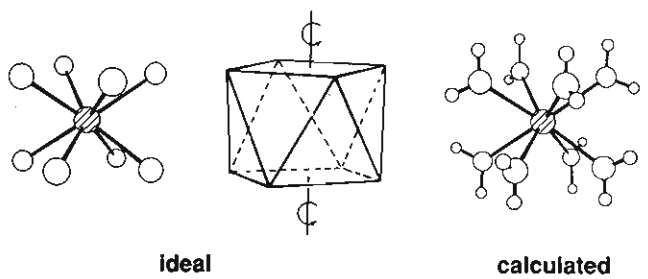

Figure 8. Ideal square antiprism and the calculated lowest energy structure for the octaaqua ion.

Table V. Comparison of Calculated and Observed M–O Bond Lengths (Å) and θ's (deg) for Octaaqua Complexes of Square-Antiprismatic Geometry

complex	M–O	θ[a]	strain energy, kJ/mol	ref
$Dy(OH_2)_8^{3+}$ (calcd)	2.373	57.5	−9.67	
$Dy(OH_2)_8Cl_3$·18-crown-6·$4H_2O$	2.386	57.0		27
$Lu(OH_2)_8^{3+}$ (calcd)	2.327	57.4	1.72	
$Lu(OH_2)_8Cl_4$·Na(12-crown-4)$_2$·$2H_2O$	2.335	57.2		28
$Lu(OH_2)_8Cl_3$·1.5(12-crown-4)·$2H_2O$	2.329	57.4		29

[a] The average of the eight angles made by the M–O bonds and the S_8 axis.

The square antiprism of D_{4d} symmetry is shown in Figure 8. In this structure the eight oxygen atoms occupy equivalent positions. The shape of the square antiprism is defined by the M–O bond length and the angle θ made by an M–O bond and the S_8 axis. Of the known structures, $Lu(OH_2)_8Cl_4Na(12\text{-crown-}4)_2\cdot 2H_2O$ contains an octaaqua ion closest to this geometry.[28] Two other structures, $Lu(OH_2)_8Cl_3\cdot 1.5(12\text{-crown-}4)\cdot 2H_2O$[29] and $Dy(OH_2)_8Cl_3\cdot 18\text{-crown-}6\cdot 4H_2O$,[27] contain octaaqua ions that can be viewed as having a distorted square-antiprismatic geometry. Comparisons of calculated and observed values of M–O bond lengths and θ are given in Table V. An excellent agreement between the observed and calculated structural features was obtained.

An ideal dodecahedron of D_{2d} symmetry is shown in Figure 9. In this structure there are two types of sites indicated as O_A and O_B. The shape of this dodecahedron is defined by the ratio of M–O_A to M–O_B bond lengths, the angle θ_A made by an M–O_A

(51) Hoard, J. L.; Silverton, J. V. *Inorg. Chem.* **1963**, *2*, 235.

Table VI. Comparison of Calculated and Observed M–O Bond Lengths (Å) and Angles (deg) for Octaaqua Complexes of Dodecahedral Geometry

complex	$M-O_A$	$M-O_B$	θ_A[a]	θ_B[b]	strain energy, kJ/mol	ref
$Gd(OH_2)_8^{3+}$ (calcd)	2.433	2.344	34.4	74.3	−12.47	
$Gd(OH_2)_8Cl_3 \cdot 2C_{10}H_8N_2$	2.451	2.354	33.9	75.9		30
$Gd(OH_2)_8Cl_3$·15-crown-5	2.433	2.390	36.8	71.8		31
$Lu(OH_2)_8^{3+}$ (calcd)	2.384	2.258	34.6	74.5	1.92	
$Lu(OH_2)_8Cl_3$·15-crown-5	2.376	2.318	36.4	71.7		31

[a] The average of the four angles made by the $M-O_A$ bonds and the S_4 axis. [b] The average of the four angles made by the $M-O_B$ bonds and the S_4 axis.

bond and the S_4 axis, and the angle θ_B made by an $M-O_B$ bond and the S_4 axis. In order to obtain this geometry with the aqua ligands, it was necessary to impose symmetry constraints. One oxygen atom of each type was related to the other three by an S_4 symmetry axis. The resulting calculated structure, shown in Figure 9, was only slightly higher in energy, 0.2–0.8 kJ/mol, than the corresponding square-antiprism isomer. Of the known structures, $Gd(OH_2)_8Cl_3 \cdot 2C_{10}H_8N_2$ contains an octaaqua ion closest to this geometry.[30] Two other structures, $Gd(OH_2)_8Cl_3$·15-crown-5[31] and $Lu(OH_2)_8Cl_3$·15-crown-5,[31] contain octaaqua ions described as "distorted" dodecahedra. Comparisons of observed and calculated structural features are given in Table VI. While the agreement between the calculated and observed structures is good for the Gd ion which exhibits a near ideal dodecahedral geometry,[30] the distorted dodecahedra[31] have $M-O_B$ bond lengths longer than those predicted by the calculations.

(iii) Complexes Containing Aqua and/or Nitrato Ligands. Structural data are available for 19 monometallic lanthanide(III) complexes with inner coordination spheres consisting of nitrato or mixed aqua and nitrato ligands.[32-47] A total of 10 geometries are represented about these 9- to 12-coordinate metal ions. It was possible to reproduce all of these by MM2 calculations. Representative examples of observed and calculated structures are shown in Figures 10–13. It was not possible to compare hydrogen atom positions, since they are not given for the observed structures, and therefore, the hydrogen atoms are not shown in the calculated structures.

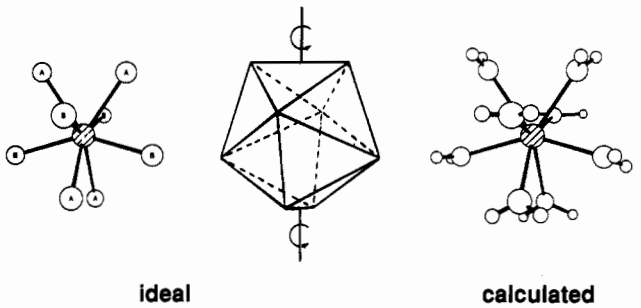

Figure 9. Ideal dodecahedron and the calculated dodecahedral structure for the octaaqua ion.

A comparison of calculated and observed average structural features is presented in Table VII. With few exceptions, calculated average $M-O_{nit}$ (nit = nitrato) bond lengths are within ±0.02 Å of observed values and calculated $M-O_{aqua}$ bond lengths are within ±0.03 Å of observed values. The average discrepancy between calculated and observed O–M–O angles is ≤3°. The calculated nitrato intraligand geometry was constant from complex to complex with the following bond lengths and angles: N—O, 1.255 Å; N═O, 1.219 Å; O—M—O, 116.8°; O—N═O, 121.6°. The nitrogen–oxygen bond lengths are within ±0.02 Å of observed values, and angles about the nitrogen are within ±2° of the observed values.

Table VII. Comparison of Observed and Calculated Average Bond Lengths (Å) and Angle Deviations (deg) for the Nitrato- and Mixed Aqua- and Nitratolanthanide(III) Complexes[a]

complex	av $M-O_{nit}$[b]	av $M-O_{aqua}$	av O–M–O angle deviation	strain energy, kJ/mol	ref
$[La(NO_3)_3(OH_2)_5] \cdot H_2O$	2.731	2.579	1.9		32
	[2.723]	[2.583]		[−10.88]	
$K_2[La(NO_3)_5(OH_2)_2]$	2.681	2.697	1.5		33
	[2.696]	[2.639]		[−5.82]	
$(NH_4)_2[La(NO_3)_5(OH_2)_2] \cdot 2H_2O$	2.694	2.591	1.3		34
	[2.701]	[2.601]		[−8.24]	
$(NH_4)_2[La(NO_3)_5(OH_2)_2] \cdot H_2O$	2.697	2.541	1.4		34
	[2.701]	[2.601]		[−8.24]	
$(Mg(OH_2)_6)_3[La(NO_3)_6]_2 \cdot 6H_2O$	2.655		1.3		35a
	[2.665]			[−7.32]	
$((C_6H_5)_3C_2H_5P)_2[Ce(NO_3)_5]$	2.567		2.2		36
	[2.532]			[−12.64]	
$[Ce(NO_3)_3(OH_2)_5] \cdot H_2O$	2.714	2.547	2.0		37
	[2.715]	[2.558]		[−7.28]	
$(Mg(OH_2)_6)_3[Ce(NO_3)_6]_2 \cdot 6H_2O$	2.657		1.4		38
	[2.653]			[−4.98]	
$[Pr(NO_3)_3(OH_2)_4] \cdot 2H_2O$	2.617	2.467	2.0		39a
	[2.597]	[2.474]		[−13.72]	
$[Nd(NO_3)_3(OH_2)_4] \cdot 2H_2O$	2.601	2.447	1.8		40
	[2.591]	[2.459]		[−12.22]	
$(Nd(NO_3)(C_{18}H_{36}N_2O_6))[Nd(NO_3)_5(OH_2)]$	2.580	2.539	2.7		41
	[2.592]	[2.480]		[−6.49]	
$(Nd_3(C_{36}H_{72}N_6O_{36}))[Nd(NO_3)_6]$	2.59				42
	[2.640]			[−0.29]	
$(Sm(NO_3)(C_{18}H_{36}N_2O_6))[Sm(NO_3)_5(OH_2)]$	2.553	2.493	2.7		43
	[2.567]	[2.460]		[−1.00]	
$[Gd(NO_3)_3(OH_2)_3] \cdot C_{12}H_{24}O_6$	2.451	2.395	3.2		44
	[2.449]	[2.349]		[−11.76]	
$[Dy(NO_3)_3(OH_2)_3] \cdot C_{15}H_{22}O_5$	2.450	2.346	2.6		45
	[2.440]	[2.326]		[−8.70]	
$(NO)_2[Ho(NO_3)_5]$	2.448		2.5		46
	[2.439]			[−1.67]	
$K_2[Er(NO_3)_5]$	2.431		2.3		47
	[2.432]			[−0.08]	

[a] Calculated values are given in parentheses. [b] Nit = nitrato.

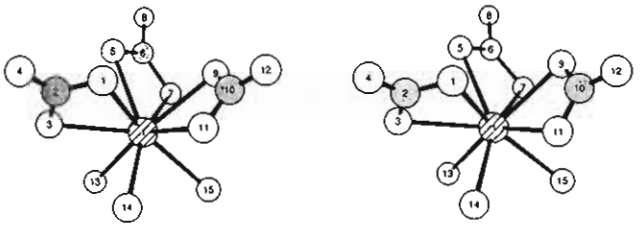

observed calculated

Figure 10. Observed[45] and calculated structures of $Dy(OH_2)_3(NO_3)_3$. Selected bond lengths and angles are listed. Calculated values are given in parentheses after the observed values. Bond lengths (Å) involving the Dy atom are as follows: O(1), 2.437 (2.417); O(3), 2.468 (2.462); O(5), 2.423 (2.416); O(7), 2.455 (2.458); O(9), 2.420 (2.422); O(11), 2.494 (2.468); O(13), 2.374 (2.325); O(14), 2.319 (2.327). Bond angles (deg) involving the Dy atom are as follows: O(1)–Dy–O(3), 51.9 (51.9); O(1)–Dy–O(5), 73.4 (78.0); O(1)–Dy–O(9), 83.4 (78.3); O(1)–Dy–O(11), 70.4 (73.6); O(3)–Dy–O(5), 73.8 (73.5); O(3)–Dy–O(13), 72.5 (73.9); O(3)–Dy–O(14), 77.2 (74.6); O(5)–Dy–O(7), 52.0 (51.9); O(5)–Dy–O(13), 90.6 (86.1); O(7)–Dy–O(9), 69.7 (73.6); O(7)–Dy–O(13), 69.7 (73.6); O(7)–Dy–O(13), 77.1 (74.8); O(7)–Dy–O(15), 76.8 (74.1); O(9)–Dy–O(11), 51.6 (51.7); O(9)–Dy–O(15), 83.0 (86.0); O(11)–Dy–O(14), 74.2 (73.8); O(11)–Dy–O(15), 80.1 (74.6); O(13)–Dy–O(14), 80.3 (81.0); O(13)–Dy–O(15), 79.9 (80.8); O(14)–Dy–O(15), 77.0 (80.9).

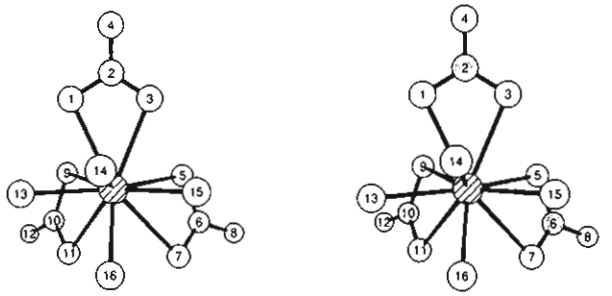

observed calculated

Figure 11. Observed[39a] and calculated structures of $Pr(NO_3)_3(OH_2)_4$. Selected bond lengths and angles are listed. Calculated values are given in parentheses after the observed values. Bond lengths (Å) involving the Pr atom are as follows: O(1), 2.555 (2.606); O(3), 2.579 (2.577); O(5), 2.636 (2.587); O(7), 2.600 (2.620); O(9), 2.611 (2.574); O(11), 2.720 (2.616); O(13), 2.470 (2.485); O(14), 2.452 (2.482); O(15), 2.470 (2.485); O(16), 2.474 (2.442). Bond angles (deg) involving the Pr atom are as follows: O(1)–Pr–O(3), 48.6 (48.6); O(1)–Pr–O(9), 68.4 (67.8); O(1)–Pr–O(13), 69.7 (70.7); O(3)–Pr–O(5), 69.0 (67.6); O(3)–Pr–O(14), 78.6 (77.8); O(3)–Pr–O(15), 69.4 (72.7); O(5)–Pr–O(7), 48.2 (48.4); O(5)–Pr–O(9), 70.7 (68.3); O(5)–Pr–O(11), 88.2 (84.4); O(5)–Pr–O(15), 75.8 (76.1); O(7)–Pr–O(9), 87.1 (89.9); O(7)–Pr–O(11), 66.1 (66.4); O(7)–Pr–O(15), 70.0 (69.4); O(7)–Pr–O(16), 71.9 (71.0); O(9)–Pr–O(11), 47.3 (48.6); O(9)–Pr–O(13), 74.4 (78.7); O(11)–Pr–O(13), 69.6 (69.5); O(11)–Pr–O(16), 70.2 (75.8); O(13)–Pr–O(14), 70.5 (72.0); O(13)–Pr–O(16), 78.8 (75.4); O(14)–Pr–O(15), 70.7 (70.4); O(14)–Pr–O(15), 70.7 (70.4); O(14)–Pr–O(16), 75.4 (78.9); O(15)–Pr–O(16), 79.5 (78.1).

While there is reasonably good agreement between the calculated and observed average structural features given in Table VII, the ability to closely reproduce the individual bond lengths is variable. For example, in the TCTP complex $Dy(NO_3)_3(H_2O)_3$ (Figure 10) calculations reproduce all three long and three short $M–O_{nit}$ bond lengths to within ±0.03 Å and all three $M–O_{aqua}$ bond lengths to within ±0.03 Å. However, in the complex $La(NO_3)_3(OH_2)_5$ (Figure 12), where the calculated average $M–O_{nit}$ and $M–O_{aqua}$ bond lengths agree to within ±0.010 Å of the observed values, the discrepancies in individual M–O bond lengths are as large as 0.09 Å.

The discrepancies between calculated and observed structure once again raise questions concerning the influence of crystal lattice effects. The two structures of $(NH_4)_2La(NO_3)_5(OH_2)_2$ provide

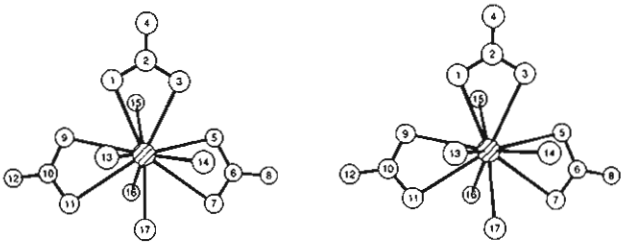

observed calculated

Figure 12. Observed[32] and calculated structures of $La(NO_3)_3(OH_2)_5$. Selected bond lengths and angles are listed. Calculated values are given in parentheses after the observed values. Bond lengths (Å) involving the La atom are as follows: O(1), 2.700 (2.700); O(3), 2.687 (2.706); O(5), 2.617 (2.694); O(7), 2.845 (2.768); O(9), 2.659 (2.682); O(11), 2.875 (2.798); O(13), 2.554 (2.587); O(14), 2.668 (2.575); O(15), 2.585 (2.595); O(16), 2.527 (2.566); O(17), 2.560 (2.590). Bond angles (deg) involving the La atom are as follows: O(1)–La–O(3), 47.2 (46.5); O(1)–La–O(9), 62.4 (64.4); O(1)–La–O(13), 65.6 (64.7); O(1)–La–O(15), 69.3 (71.9); O(3)–La–O(5), 65.2 (62.9); O(3)–La–O(14), 65.8 (65.4); O(3)–La–O(15), 72.4 (69.3); O(5)–M–O(7), 46.0 (45.9); O(5)–La–O(14), 73.9 (72.7); O(5)–La–O(15), 66.4 (66.1); O(5)–La–O(16), 80.7 (84.2); O(7)–La–O(14), 64.9 (70.3); O(7)–La–O(16), 68.1 (65.1); O(7)–La–O(17), 64.5 (63.4); O(9)–La–O(11), 45.7 (45.8); O(9)–La–O(13), 75.9 (79.2); O(9)–La–O(15), 67.2 (66.8); O(9)–La–O(16), 75.6 (74.2); O(11)–La–O(13), 69.2 (65.8); O(11)–La–O(16), 63.0 (65.3); O(11)–La–O(17), 60.9 (63.2); O(13)–La–O(14), 73.5 (71.3); O(13)–La–O(17), 70.1 (70.8); O(14)–La–O(17), 70.5 (71.4); O(15)–La–O(16), 68.2 (70.8); O(16)–La–O(17), 81.4 (78.9).

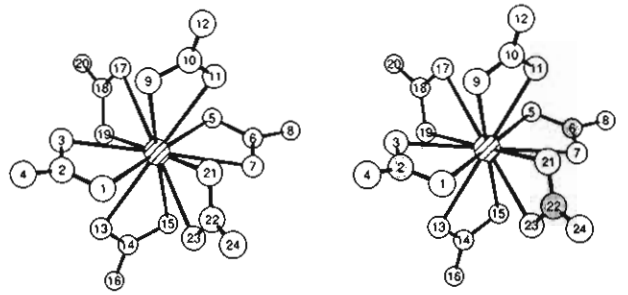

observed calculated

Figure 13. Observed[35a] and calculated structures of the $La(NO_3)_6^{3-}$ ion. Selected bond lengths and angles are listed. Calculated values are given in parentheses after the observed values. Bond lengths (Å) involving the La atom are as follows: O(1), 2.639 (2.665); O(3), 2.647 (2.664); O(5), 2.636 (2.665); O(7), 2.697 (2.670); O(9), 2.647 (2.674); O(11), 2.639 (2.654); O(13), 2.636 (2.664); O(15), 2.697 (2.673); O(17), 2.647 (2.660); O(19), 2.639 (2.670); O(21), 2.636 (2.657); O(23), 2.698 (2.664). Bond angles (deg) involving the La atom are as follows: O(1)–La–O(3), 47.4 (47.2); O(1)–La–O(9), 71.8 (68.7); O(1)–La–O(13), 67.6 (68.9); O(1)–La–O(21), 66.7 (68.6); O(1)–La–O(23), 66.6 (68.5); O(3)–La–O(9), 69.8 (68.7); O(3)–La–O(13), 67.8 (68.9); O(3)–La–O(17), 69.8 (68.4); O(3)–La–O(19), 71.8 (68.3); O(5)–La–O(7), 46.9 (47.2); O(5)–La–O(11), 66.7 (68.1); O(5)–La–O(15), 70.0 (68.2); O(5)–La–O(17), 67.8 (68.4); O(5)–La–O(19), 67.6 (68.3); O(7)–La–O(11), 66.6 (68.1); O(7)–La–O(15), 68.0 (68.2); O(7)–La–O(21), 69.9 (68.6); O(7)–La–O(23), 68.0 (68.5); O(9)–La–O(11), 47.4 (47.1); O(9)–La–O(17), 69.8 (67.8); O(9)–La–O(21), 67.8 (67.8); O(11)–La–O(17), 71.8 (67.8); O(11)–La–O(21), 67.6 (67.9); O(13)–La–O(15), 46.9 (47.3); O(13)–La–O(19), 66.7 (69.0); O(13)–La–O(23), 70.0 (69.1); O(15)–La–O(19), 66.6 (69.2); O(15)–La–O(23), 70.0 (69.1); O(17)–La–O(19), 47.4 (47.2); O(21)–La–O(23), 45.9 (47.3).

an example of how a minor change in the crystal environment can influence structure.[34] In one of these structures the complex crystallizes with 1 equiv of water, while, in the other structure, 2 equiv of water is present. The presence of the extra lattice water causes changes of up to 0.023 Å in $M–O_{nit}$ bond length, 0.052 Å in $M–O_{aqua}$ bond length, and 3° in O–M–O angle. In this example, the largest change in structure involves the aqua ligand. This is not surprising given its propensity for hydrogen bonding.

It is probably for this reason that the discrepancies between observed and calculated average M–O bond lengths are, in general, larger for the aqua ligands than for the nitrato ligands.

Calculated strain energy values are also given in Table VII. The negative values are due to the fact that the amount of strain resulting from steric repulsion in the inner coordination sphere is more than compensated for by the numerous long-range attractive van der Waals interactions. Comparisons reveal only small differences in energy for the structural isomers present in Table VII. The NH_4^+ isomer of $La(NO_3)_5(OH_2)_2^{2-}$ is only 2.5 kJ/mol lower in energy than the K^+ isomer. Even smaller differences are observed when calculations are carried out for the same metal ion in the two configurations of $M(NO_3)_3(OH_2)_3$ (the Gd form is 0.4 kJ/mol lower in energy than the Dy form) and in the two configurations of $M(NO_3)_5(OH_2)^{2-}$ (the Nd form is 0.08 kJ/mol lower in energy than the Sm form).

Summary

This study shows how molecular mechanics methodology can be successfully applied to the calculation of structure in high-coordinate metal complexes. A simple method based on the replacement of L–M–L bending interactions with nonbonded interactions between the ligand donor atoms and the use of harmonic M–L stretching potentials yields very reasonable geometric results. The method has been tested by generating 58 known structures of the aqua- and nitratolanthanide(III) complexes. In the majority of cases the discrepancies between observed and calculated M–O bond lengths and O–M–O bond angles are ≤0.03 Å (≤1–2%) and ≤3°, respectively. Larger discrepancies can be traced to lattice distortions in the observed structures, which are not included in the model.

Although this study has focused on modeling geometries found in high-coordinate metal complexes, the methodology is not limited to the f-block metals. Force fields based on repulsions between ligand donor atoms are suitable models for many of the more common geometries encountered in coordination compounds.[12-16] The MM2 implementation of this type of force field can be used to generate the important tetrahedral, trigonal-bipyramidal, and octahedral geometries found in transition-metal complexes. Square-planar and square-pyramidal geometries can also be obtained.[52] This approach provides a useful alternative to the conventional molecular mechanics force fields that rely upon the definition of strain-free L–M–L bond angles.

Acknowledgment. I acknowledge financial support provided by a Director's Postdoctoral Fellowship at Los Alamos National Laboratory. I am grateful to Dr. Robert R. Ryan, Dr. Alfred P. Sattelberger, and Dr. David C. Smith for reading the manuscript and offering useful comments, Dr. Gordon D. Jarvinen for funding equipment and supplies, and Dr. Paul H. Smith for his invaluable assistance with computer hardware and software.

Supplementary Material Available: An example MM2 input file for $Lu(OH_2)_8^{3+}$ (1 page). Ordering information is given on any current masthead page.

(52) These two geometries can be obtained either by restricting four of the donor atoms to lie in the XY plane or by introducing lone pair(s) in the axial position(s).

Contribution from the Department of Chemistry, University of California, Davis, California 95616

Synthesis and Spectroscopic and X-ray Structural Characterization of the First Homoleptic Transition-Metal Boryloxides $[Mn(OBTrip_2)(\mu\text{-}OBTrip_2)]_2$ and $[Fe(OBMes_2)(\mu\text{-}OBMes_2)]_2$

Hong Chen, Philip P. Power,* and Steven C. Shoner

Received October 2, 1990

The reactions of the metal amides $Mn[N(SiMe_3)_2]_2$ and $Fe[N(SiMe_3)_2]_2$ with the sterically crowded boronous acids $Trip_2BOH$ and Mes_2BOH (Trip = 2,4,6-i-$Pr_3C_6H_2$, Mes = 2,4,6-$Me_3C_6H_2$) afford the compounds $[Mn(OBTrip_2)(\mu\text{-}OBTrip_2)]_2$ (**1**) and $[Fe(OBMes_2)(\mu\text{-}OBMes_2)]_2$ (**2**), which are the first two examples of homoleptic transition-metal boryloxides. The X-ray crystal structures of compounds **1** and **2** have also been determined. The data show that both **1** and **2** are dimeric with three-coordinate Mn and Fe centers that are bound to one terminal boryloxide ligand and to two bridging boryloxide ligands. The M···M distances (3.094 (5) Å for Mn and 3.057 (5) Å for Fe) are considerably longer than those found in the amide precursors. Surprisingly, the metric features of **1** and **2** are very close to those observed in the closely related bis(aryloxo) complexes $[M(OAr)_2]_2$ (Ar = 2,4,6-t-$Bu_3C_6H_2$, M = Mn (**3**), Fe (**4**)). This suggests that the M–O bonding in **1**–**4** is similar: furthermore, it is mainly ionic and little evidence for a π-contribution to the M–O bond could be observed. Compounds **1** and **2** have also been characterized by magnetic measurements. Crystallographic data with Mo Kα radiation (λ = 0.71069 Å) at 130 K: **1**, a = 33.898 (11) Å, b = 16.985 (5) Å, c = 30.861 (11) Å, β = 134.65 (2)°, Z = 4, R = 0.088, space group $C2/c$; **2**, a = 15.004 (5) Å, b = 14.957 (4) Å, c = 16.915 (6) Å, β = 93.86 (3)°, Z = 2, R = 0.074, space group $P2_1/n$.

Introduction

The increasing availability of detailed knowledge of the structures and reactivity of molecular transition-metal alkoxides and aryloxides has, with a few important exceptions, been concerned with the early metals.[1-5] For example, if homoleptic alkoxides or aryloxides of formula $[M(OR)_n]$ (n = 2, 3, etc; M = Mn, Fe, Co, Ni, Cu) are considered, only a small number of these or related complexes have been well characterized. Spectroscopic and analytical data have appeared for a few species such as $[LiFe(OR)_4]$, $[Co(OR)_2]_2$ (R = $CH(t\text{-}Bu)_2$ or 1-adamantyl).[6,7]

(1) Bradley, D. C.; Mehrotra, R. C.; Gaur, D. P. *Metal Alkoxides*, Academic Press: New York, 1978.
(2) Mehrotra, R. C. *Adv. Inorg. Chem.* **1983**, *26*, 269.
(3) Rothwell, I. P. *Acc. Chem. Res.* **1988**, *21*, 153.
(4) Hvoslef, J.; Hope, H.; Murray, B. D.; Power, P. P. *J. Chem. Soc., Chem. Commun.* **1983**, 1438.
(5) Lubben, T. V.; Wolczanski, P. T.; Van Duyne, G. D. *Organometallics* **1984**, *3*, 977.
(6) Bochmann, M.; Wilkinson, G.; Young, G. B.; Hursthouse, M. B.; Malik, K. M. A. *J. Chem. Soc., Dalton Trans.* **1980**, 901.
(7) Bochmann, M.; Wilkinson, G.; Young, G. B.; Hursthouse, M. B.; Malik, K. M. A. *J. Chem. Soc., Dalton Trans.* **1980**, 1863.

0020-1669/91/1330-2884$02.50/0